

Two Novel Copper–Undecaniobates Decorated by Copper–Organic Cations $[\{\text{Cu}(\text{H}_2\text{O})\text{L}\}_2\{\text{CuNb}_{11}\text{O}_{35}\text{H}_4\}]^{5-}$ ($\text{L} = 1,10\text{-phenanthroline}, 2,2'\text{-bipyridine}$) Consisting of Plenary and Monolacunary Lindqvist-Type Isopolyniobate Fragments

Jing-Yang Niu,^[a] Guo Chen,^[a] Jun-Wei Zhao,^[a] Peng-Tao Ma,^[a] Su-Zhi Li,^[a] Jing-Ping Wang,^{*[a]} Ming-Xue Li,^[a] Yan Bai,^[a] and Bian-Sheng Ji^[b]

Polyoxoniobates (PONs) have attracted increasing interest in the past several decades because their unique high basicity and high surface charge characteristics endow them potential applications in various fields such as nuclear-waste treatment, virology, and base-catalyzed decomposition of biocontaminants.^[1] In comparison with polyoxotungstates, -molybdates and -vanadates,^[2] PONs remains largely unexplored due to the low activity of niobium species. Most of known PON species contain the Lindqvist-type polyoxoanion units $[\text{Nb}_6\text{O}_{19}]^{8-}$.^[1c,3] Nyman et al. reported several Keggin-type heteropolyniobates $[\text{XNb}_{12}\text{O}_{40}]^{y-}$ ($\text{X} = \text{Si}^{\text{IV}}, \text{Ge}^{\text{IV}}, \text{P}^{\text{V}}, \text{y} = 15, 16$) and their derivatives $[\text{H}_2\text{Si}_4\text{Nb}_{16}\text{O}_{56}]^{14-}$ and $[(\text{PO}_2)_3\text{PNb}_9\text{O}_{34}]^{15-}$,^[4] as well as a large isopolyniobate $[\text{Nb}_{24}\text{O}_{72}\text{H}_6]^{15-}$ cluster and a family of copper-linked hexaniobate clusters.^[1d,5] Other PON clusters have also been reported.^[6] In 2007, our group prepared a family of giant PON clusters and a hexaniobate monomer decorated by $[\text{Cu}(2,2'\text{-bipy})_x]^{2+}$ ($x = 1, 2$),^[7] which showed that the combination of transition-metal complexes and the precursor $[\text{Nb}_6\text{O}_{19}]^{8-}$ in basic media provided a quite effective way for synthesizing novel PONs. Here, by introducing aromatic amine ligands (1,10-phenanthroline = phen, 2,2'-bipyridine = 2,2'-bipy) and

Cu^{2+} ion into the $[\text{Nb}_6\text{O}_{19}]^{8-}$ system to construct organic–inorganic hybrid PONs, we have obtained two hybrid copper–undecaniobates $\text{K}_3\text{Na}_2[\{\text{Cu}(\text{H}_2\text{O})(\text{phen})\}_2\{\text{CuNb}_{11}\text{O}_{35}\text{H}_4\} \cdot 22\text{H}_2\text{O}$ (**1**) and $\text{K}_4\text{Na}[\{\text{Cu}(\text{H}_2\text{O})(2,2'\text{-bipy})\}_2\{\text{CuNb}_{11}\text{O}_{35}\text{H}_4\} \cdot 25\text{H}_2\text{O}$ (**2**), each containing a novel $[\text{CuNb}_{11}\text{O}_{35}\text{H}_4]^{9-}$ (abbreviated as $\{\text{CuNb}_{11}\}$) cluster consisting of plenary and monolacunary Lindqvist-type isopolyniobate fragments, which also demonstrate impressive antitumor activities. To our knowledge, both **1** and **2** represent the first examples of copper–undecaniobates. To date, no such analogue is observed in vanadium, molybdenum, or tungsten oxide clusters.

Clusters **1** and **2** were synthesized by using the diffusion strategy with the reaction involving $\text{K}_7\text{HNb}_6\text{O}_{19} \cdot 13\text{H}_2\text{O}$, $\text{Cu}(\text{NO}_3)_2 \cdot 3\text{H}_2\text{O}$, phen/2,2'-bipy, NaOH, and H_2O . X-ray structural analyses^[8] indicate that both **1** and **2** contain a similar copper–undecaniobate cluster $\{\text{CuNb}_{11}\}$ decorated by two $[\text{Cu}(\text{H}_2\text{O})\text{L}]$ ($\text{L} = \text{phen}$ (**1**), 2,2'-bipy (**2**)) building blocks linked to the cluster through two bridging oxygen and two terminal oxygen atoms (Figure 1a,b and Figures S1 and S2 in the Supporting Information). Therefore, only the structure of **1** is described in detail here. The undecaniobate cluster $[\text{Nb}_{11}\text{O}_{35}\text{H}_4]^{11-}$ can be described as the fusion of a plenary Lindqvist $[\text{Nb}_6\text{O}_{19}]^{8-}$ fragment and a monolacunary Lindqvist $[\text{Nb}_5\text{O}_{18}]^{11-}$ fragment by corner-sharing two oxygen atoms (Figure 1c,d). The Lindqvist $[\text{Nb}_6\text{O}_{19}]^{8-}$ unit is a well-known polyoxometalate (POM) structure, first reported in 1953 by Lindqvist,^[3a] whereas the $[\text{Nb}_5\text{O}_{18}]^{11-}$ fragment is derived from a plenary Lindqvist $[\text{Nb}_6\text{O}_{19}]^{8-}$ unit by removal of one $\{\text{NbO}\}$ group (Figure S3). Although monolacunary Lindqvist $[\text{W}_5\text{O}_{18}]^{6-}$ and $[\text{Mo}_5\text{O}_{18}]^{6-}$ fragments have been discovered in some POMs,^[2a,9] the monolacunary Lindqvist $[\text{Nb}_5\text{O}_{18}]^{11-}$ fragment in **1** and **2** has never been observed to date. Charge-balance considerations of **1** indicate that there must be four protons per $[\text{Nb}_{11}\text{O}_{35}]$ unit (i.e., $[\text{Nb}_{11}\text{O}_{35}\text{H}_4]^{11-}$). Moreover, bond valence sum (BVS)^[10] cal-

[a] Prof. Dr. J.-Y. Niu, G. Chen, Dr. J.-W. Zhao, P.-T. Ma, Dr. S.-Z. Li, Prof. J.-P. Wang, Dr. M.-X. Li, Dr. Y. Bai
Institute of Molecular and Crystal Engineering
College of Chemistry and Chemical Engineering
Henan University, Kaifeng, Henan 475004 (PR China)
Fax: (+86)378-3886876
E-mail: jpwang@henu.edu.cn
jyniu@henu.edu.cn

[b] Prof. B.-S. Ji
College of Pharmacy, Henan University
Kaifeng, Henan 475004 (PR China)

Supporting information for this article is available on the WWW under <http://dx.doi.org/10.1002/chem.201000824>.

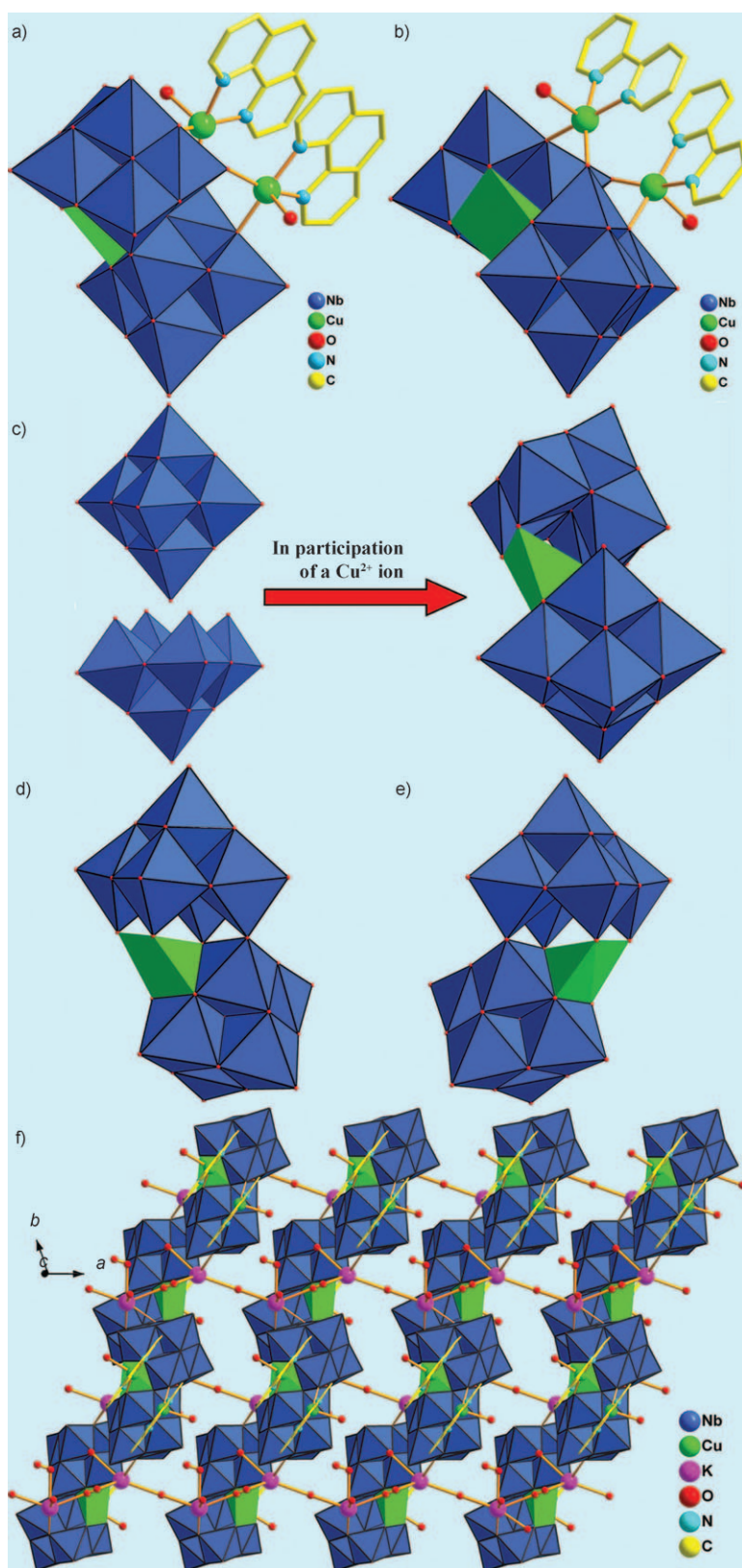


Figure 1. Polyhedral/ball-and-stick views of the anions of a) **1** and b) **2**. c) Combination of a plenary Lindqvist $[\text{Nb}_6\text{O}_{19}]^{8-}$ fragment, a monolacunary Lindqvist $[\text{Nb}_5\text{O}_{18}]^{11-}$ fragment and a Cu^{2+} ion forming the copper-undecaniobate $\{\text{CuNb}_{11}\}$ cluster. d) and e) Comparison of the $\{\text{CuNb}_{11}\}$ clusters in **1** and **2**, respectively. f) The 2D layer formed by $[\{\text{Cu}(\text{H}_2\text{O})(\text{phen})\}_2\{\text{CuNb}_{11}\text{O}_{35}\text{H}_4\}]^{5-}$ hybrid clusters with the help of K^+ ions in **1** viewed along the c -axis.

culations give the BVS values of 1.43, 1.45, 1.09, and 1.03 for O5, O7, O12, and O21 atoms in $\{\text{CuNb}_{11}\}$ unit, respectively, which are significantly lower than 2, suggesting the most probable positions for binding protons. It is very common to see protons that are localized on the surface of polyoxoanions in POM chemistry.^[1d,3d,11] In addition, in order to enhance the stability of the undecaniobate $[\text{Nb}_{11}\text{O}_{35}\text{H}_4]^{11-}$ cluster, a Cu^{2+} ($\text{Cu}1$) ion is incorporated into the pocket surrounded by the $[\text{Nb}_6\text{O}_{19}]^{8-}$ and $[\text{Nb}_5\text{O}_{18}]^{11-}$ units. The $\text{Cu}1$ cation exhibits a five-coordinate distorted square-pyramidal geometry, in which O12, O21, O28, and O32 atoms build the square plane ($\text{Cu}-\text{O}$: 1.898(7)–2.128(6) Å) and O33 atom occupies the apical positions ($\text{Cu}-\text{O}$: 2.364(6) Å).

As shown in Figure 1a and Figure S1 in the Supporting Information, two $[\text{Cu}(\text{H}_2\text{O})(\text{phen})]^{2+}$ units cap to the $\{\text{CuNb}_{11}\}$ cluster in twin fashion by means of two bridging oxygen and two terminal oxygen atoms forming a hybrid cluster $[\{\text{Cu}(\text{H}_2\text{O})(\text{phen})\}_2\{\text{CuNb}_{11}\text{O}_{35}\text{H}_4\}]^{5-}$. Similar to the $\text{Cu}1$ cation, both $\text{Cu}2$ and $\text{Cu}3$ cations in the $[\text{Cu}(\text{H}_2\text{O})(\text{phen})]^{2+}$ twin units also exhibit five-coordinate square pyramid, in which the square plane is defined by two N atoms from a phen ligand and two O atoms from the $\{\text{CuNb}_{11}\}$ unit ($\text{Cu}-\text{N}$: 1.999(8)–2.020(7) Å, $\text{Cu}-\text{O}$: 1.913(6)–1.946(6) Å), and one coordinate water occupies the apical site ($\text{Cu}-\text{O}_w$: 2.280(8)–2.321(8)). The dihedral angle between the two phen planes in the two $[\text{Cu}(\text{H}_2\text{O})(\text{phen})]$ twin units is 1.325(3)°, indicating that these two planes are approximately parallel. Furthermore, the distance between the two planes is about 3.7 Å, suggesting that there are face-to-

face π - π interactions between the two phen ligands; these interactions will also contribute to the stability of **1**. In addition, **1** can be considered as an infinitely extended 2D layer built by $[\{\text{Cu}(\text{H}_2\text{O})(\text{phen})\}_2\{\text{CuNb}_{11}\text{O}_{35}\text{H}_4\}]^{5-}$ units through K2 and K3 bridges (Figure 1 f and Figures S4 and S5 in the Supporting Information). Similar to **1**, the structure of **2** can be also considered as an extended 2D network (Figures S6–S8 in the Supporting Information).

As far as we know, the $\{\text{CuNb}_{11}\}$ clusters in **1** and **2** are the first examples of copper–undecaniobate clusters. Different from the typical PON clusters reported previously (Figure S9–S13 in the Supporting Information),^[14,4,6,7] clusters **1** and **2** contain monolacunary Lindqvist $[\text{Nb}_5\text{O}_{18}]^{11-}$ fragments. On the other hand, the $\{\text{CuNb}_{11}\}$ cluster is decorated by two copper–organic complexes, forming two novel hybrids $[\{\text{Cu}(\text{H}_2\text{O})(\text{phen})\}_2\{\text{CuNb}_{11}\text{O}_{35}\text{H}_4\}]^{5-}$ and $[\{\text{Cu}(\text{H}_2\text{O})(2,2'\text{-bipy})\}_2\{\text{CuNb}_{11}\text{O}_{35}\text{H}_4\}]^{5-}$. The above two organic–inorganic hybrid clusters are a result of a new synthetic route of incorporating other larger aromatic ligands into PON systems to construct larger structures or multidimensional heteropolyniobates. More interestingly, although both **1** and **2** crystallize in the triclinic achiral space group $P\bar{1}$, the $\{\text{CuNb}_{11}\}$ clusters in the two compounds are not identical; instead, they are enantiomers (Figure 1 d,e). Considering the potential applications of chiral POMs in medicine, nonlinear optics, and catalysis,^[12] we plan to firstly separate the $\{\text{CuNb}_{11}\}$ clusters by mean of the recognition role of chiral amino acids, thereby, making the chirality of the polyoxoanions transfer to the whole framework constructing novel PONs. This explorative work is in progress.

Thermogravimetric analyses on **1** and **2** indicate that both **1** and **2** show two steps of weight loss (Figure S14 in the Supporting Information). For **1**, the first weight loss of 14.47% from 25 to 221 °C corresponds to the release of 22 lattice water molecules. The second weight loss of 15.93% up to 453 °C is ascribed to the removal of two coordinated water ligands, two phen ligands, and the dehydration of four protons. For **2**, the first-step weight loss of 16.63% between 25 and 211 °C involves the loss of 25 lattice water molecules, followed by the loss of 14.37%, assigned to the removal of two coordinated water ligands, two bipy ligands, and the dehydration of four protons. Surface photovoltage spectroscopy (SPS) and electric-field-induced surface photovoltage spectroscopy (EFISPS) of **1** and **2** were measured to investigate their photoelectric properties under external electric fields. Figure S15 (Supporting Information) shows the EFISPS of **1** and **2** in the range of 300–600 nm under external electric fields (–2, –1, 0, +1, +2 V). The variations of SPS response intensity under external electric fields show that increasing positive electric field increases the surface photovoltage (SPV) response intensity, while the SPV response intensity decreases with decreasing the negative electric fields, indicating that **1** and **2** are n-type conductors.^[13]

UV/Vis spectra of **1** and **2** (Figure S16, S17 in the Supporting Information) in aqueous solution display four absorption bands centered at about 193, 223, 267, 664 nm for **1** and 198, 221, 300, 656 nm for **2**. The higher energy absorp-

tion bands (193, 223 nm for **1** and 198, 221 nm for **2**) are tentatively assigned to the O→Nb charge-transfer transitions, whereas the lower energy band (267 nm for **1**, 300 nm for **2**) is attributed to ligand-to-metal (Cu^{II}) charge-transfer (LMCT) transitions^[14] in comparison with UV spectra of the copper complexes. The absorption band in visible region (664 nm for **1**, 656 nm for **2**) results from the Cu^{II} d–d transitions. Cyclic voltammetry measurements of **1**, **2**, and the precursors in 0.5 M KCl aqueous solution all exhibit one pair of well-defined redox waves in the potential range of –1.0 to +1.0 V, which result from the cooperation of the redox processes of the Nb^{V} atoms and $[\text{Cu}(\text{H}_2\text{O})\text{L}]^{2+}$ ions (Figure S18 and Table S1 in the Supporting Information). Additionally, CV curves of **1** and **2** in 0.5 M KCl at different scan rates were measured (Figure S19 in the Supporting Information). It can be clearly observed that the peak potentials change gradually when the scan rate increases: the cathodic peak potentials shift to the negative direction and the anodic peak potentials toward the positive direction, meanwhile the peak-to-peak separation between the cathodic and anodic peaks increases, but the average peak potentials do not change. When the scan rates are lower than 220 mVs^{-1} , the peak currents are proportional to the scan rates (Figure S19c,d in the Supporting Information), indicating that the redox processes of **1** and **2** are surface-controlled.^[15]

To investigate the stability of **1** and **2** in aqueous solution, both aqueous systems are monitored by the in-situ UV studies (Figure S20 in the Supporting Information). Both **1** and **2** ($1 \times 10^{-5} \text{ molL}^{-1}$) remain stable for at least 30 days at ambient temperature, which is further confirmed by the in-situ CV curves of **1** and **2** in aqueous solution (Figure S21 in the Supporting Information). It is known that the polyoxoniobates are commonly sensitive to the pH value of the studied media, so the influences of the pH value on the stability of **1** and **2** in the aqueous solution were also elaborately probed by means of UV spectra and CV curves at different pH conditions. As depicted in Figure S22–S25 in the Supporting Information, the UV spectra and CV curves slightly change when the pH values vary in the range of 4–12, indicating that the anion frameworks of **1** and **2** are still retained. However, when the pH values are lower than 4 or higher than 12, the UV spectra and CV curves change significantly, suggesting that the polyoxoanion frameworks have been decomposed. These data indicate that **1** and **2** are stable in the pH ranges of 4–12.

Taking into account that POMs exhibit significantly biological activities,^[1a,16] we have studied the ability of inhibiting tumor cell growth for $\text{K}_7\text{HfNb}_6\text{O}_{19} \cdot 13\text{H}_2\text{O}$, **1**, and **2**, and also calculated the IC_{50} values (compound concentration that render 50% of cell death) in micromolar units (Figure 2 and Table S2 in the Supporting Information). Preliminary in vitro screening shows that both **1** and **2** exhibit remarkably higher antitumor activities (IC_{50} : $0.38 \pm 0.05 \mu\text{M}$ for **1** and $0.10 \pm 0.03 \mu\text{M}$ for **2**), while the precursor $\text{K}_7\text{HfNb}_6\text{O}_{19}$ has no effect ($\text{IC}_{50} > 100 \mu\text{M}$) against human leucocythemia cancer K562 cell line. Evidently, the introduction of the Cu^{2+} ions and organic ligand (phen and 2,2'-

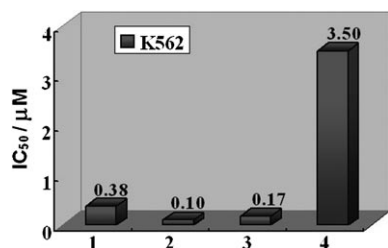


Figure 2. The antitumor activities of **1**, **2**, [Cu(phen)(NO₃)₂] (**3**) and [Cu(2,2'-bipy)(NO₃)₂] (**4**) against the human leucocythemia K562 cell line (all data represent the average values for three separate experiments).

bipy) into the hexaniobate system remarkably enhances the antitumor potency, which indicates that the Cu²⁺ ion in the copper–undecaniobate cluster and the decorative copper complex fragments in **1** and **2** play a significant role in their growth inhibitory activity.^[17] Additionally, the antitumor actions of [Cu(phen)(NO₃)₂] (**3**) and [Cu(2,2'-bipy)(NO₃)₂] (**4**) (as shown in Figure 2) further testify our hypothesis. With detailed studies, the new compounds could be helpful in designing more potent antitumor agents for further stages of screening in vitro and/or in vivo.

In summary, two organic–inorganic hybrid PONs **1** and **2** have been successfully synthesized by the diffusion strategy, representing the first copper–undecaniobates consisting of plenary and monolacunary Lindqvist-type isopolyniobate fragments. The successful syntheses of **1** and **2** enriches the structural diversity of PONs and further proves that the concept that the use of organic cations or metal–ligand cations could provide new avenues towards diversification of PON cluster geometries. In addition it provides us an enlightening synthetic strategy for the introduction of other transition-metal cations or large aromatic ligands or chiral ligands into this system to construct organic–inorganic hybrid multidimensional PONs or chiral PONs. In addition, the good solubility and stability in aqueous solution at pH 4–12 and impressive antitumor activity suggest that **1** and **2** have the potential of being antitumor agents for therapeutic use.

Experimental Section

Syntheses of 1 and 2: K₇HNb₆O₁₉·13H₂O was prepared according to the literature method^[18] and identified by IR spectra. Phen (0.099 g, 0.50 mmol)/2,2'-bipy (0.078 g, 0.50 mmol) was added to the solution of Cu(NO₃)₂·3H₂O (0.242 g, 1.00 mmol) in water (5 mL) under stirring. Then the resulting blue solution was added dropwise to the solution of K₇HNb₆O₁₉·13H₂O (1.370 g, 1.00 mmol) in water (60 mL) under stirring. Subsequently, the mixture was adjusted to pH 11.2 using NaOH (1 mol L⁻¹) solution, condensed to 30 mL at 55 °C for 8 h, filtered, and then transferred to a straight glass tube. Ethanol was carefully layered onto the resulting dark green solution (Scheme S1 in the Supporting Information). Diffusion between the two phases over a period of 3 weeks produced block-shaped light-blue single crystals of **1** or **2**.

Data for 1: Yield: 40% based on K₇HNb₆O₁₉·13H₂O; elemental analysis calcd (%) for C₂₄H₆₈ Cu₃K₃N₄Na₂Nb₁₁O₃₉: C 10.55, H 2.51, N 2.05; found: C 10.32, H 2.73, N 1.87; IR (KBr pellet): $\tilde{\nu}$ = 3393 (s), 1588 (w),

1519 (m), 1429 (m), 1146 (w), 1107 (w), 852 (s), 754 (s), 698 (s), 535 (m), 422 cm⁻¹ (m).

Data for 2: Yield: 45% based on K₇HNb₆O₁₉·13H₂O; elemental analysis calcd (%) for C₂₀H₇₄Cu₃K₄N₄NaNb₁₁O₆₂: C 8.72, H 2.71, N 2.03; found: C 8.56, H 2.89, N 1.84; IR (KBr pellet): $\tilde{\nu}$ = 3378 (s), 1601 (m), 1588 (w), 1446 (m), 1162 (w), 1107 (w), 854 (s), 750 (s), 688 (s), 535 (m), 414 cm⁻¹ (m).

Acknowledgements

This work was supported by the National Natural Science Foundation of China, the Special Research Fund for the Doctoral Program of Higher Education, Innovation Scientists and Technicians Troop Construction Projects of Henan Province, the Foundation of Education Department of Henan Province, and the Natural Science Foundation of Henan Province.

Keywords: antitumor agents • copper • niobium • organic–inorganic hybrid composites • polyoxometalates • synthetic chemistry

- [1] a) J. T. Rhule, C. L. Hill, D. A. Judd, *Chem. Rev.* **1998**, *98*, 327–357; b) A. J. Russell, J. A. Berberich, G. F. Drevon, R. R. Koepsel, *Annu. Rev. Biomed. Eng.* **2003**, *5*, 1–27; c) A. V. Besserguenev, M. H. Dickman, M. T. Pope, *Inorg. Chem.* **2001**, *40*, 2582–2586; d) R. P. Bontchev, M. Nyman, *Angew. Chem.* **2006**, *118*, 6822–6824; *Angew. Chem. Int. Ed.* **2006**, *45*, 6670–6672.
- [2] a) K. Wassermann, M. H. Dickman, M. T. Pope, *Angew. Chem.* **1997**, *109*, 1513–1516; *Angew. Chem. Int. Ed. Engl.* **1997**, *36*, 1445–1448; b) A. Müller, P. Kögerler, C. Kuhlmann, *Chem. Commun.* **1999**, 1347–1358; c) A. Müller, R. Rohlfing, J. Döring, M. Penk, *Angew. Chem.* **1991**, *103*, 575–577; *Angew. Chem. Int. Ed. Engl.* **1991**, *30*, 588–590.
- [3] a) I. Lindqvist, *Ark. Kemi* **1953**, *5*, 247–250; b) T. Ozeki, T. Yamase, H. Naruke, Y. Sasaki, *Inorg. Chem.* **1994**, *33*, 409–410; c) T. M. Alam, M. Nyman, B. R. Cherry, J. M. Segall, L. E. Lybarger, *J. Am. Chem. Soc.* **2004**, *126*, 5610–5620; d) M. Nyman, T. M. Alam, F. Bonhomme, M. A. Rodriguez, C. S. Frazer, M. E. Welk, *J. Cluster Sci.* **2006**, *17*, 197–219; e) D. Laurencin, R. Thouvenot, K. Boubekeur, A. Proust, *Dalton Trans.* **2007**, 1334–1345.
- [4] a) M. Nyman, F. Bonhomme, T. M. Alam, M. A. Rodriguez, B. R. Cherry, J. L. Krumhansl, T. M. Nenoff, A. M. Sattler, *Science* **2002**, *297*, 996–998; b) M. Nyman, F. Bonhomme, T. M. Alam, J. B. Parise, G. M. B. Vaughan, *Angew. Chem.* **2004**, *116*, 2847–2852; *Angew. Chem. Int. Ed.* **2004**, *43*, 2787–2792; c) F. Bonhomme, J. P. Larentzos, T. M. Alam, E. J. Maginn, M. Nyman, *Inorg. Chem.* **2005**, *44*, 1774–1785; d) M. Nyman, A. J. Celestian, J. B. Parise, G. P. Holland, T. M. Alam, *Inorg. Chem.* **2006**, *45*, 1043–1052; e) T. M. Anderson, S. G. Thoma, F. Bonhomme, M. A. Rodriguez, H. Park, J. B. Parise, T. M. Alam, J. P. Larentzos, M. Nyman, *Cryst. Growth Des.* **2007**, *7*, 719–723; f) T. M. Anderson, T. M. Alam, M. A. Rodriguez, J. N. Bixler, W. Q. Xu, J. B. Parise, M. Nyman, *Inorg. Chem.* **2008**, *47*, 7834–7839.
- [5] R. P. Bontchev, E. L. Venturini, M. Nyman, *Inorg. Chem.* **2007**, *46*, 4483–4491.
- [6] a) C. M. Flynn, G. D. Stucky, *Inorg. Chem.* **1969**, *8*, 332–334; b) C. M. Flynn, G. D. Stucky, *Inorg. Chem.* **1969**, *8*, 335–344; c) E. J. Graeber, B. Morosin, *Acta Crystallogr. Sect. B* **1977**, *33*, 2137–2143; d) M. Maekawa, Y. Ozawa, A. Yagasaki, *Inorg. Chem.* **2006**, *45*, 9608–9609; e) M. Nyman, L. J. Criscenti, F. Bonhomme, M. A. Rodriguez, R. T. Cygan, *J. Solid State Chem.* **2003**, *176*, 111–119; f) L. Shen, C. H. Li, Y. N. Chi, C. W. Hu, *Inorg. Chem. Commun.* **2008**, *11*, 992–994; g) C. A. Ohlin, E. M. Villa, J. C. Fettinger, W. H. Casey, *Angew. Chem.* **2008**, *120*, 5716–5718; *Angew. Chem. Int. Ed.* **2008**, *47*, 5634–5636; h) R. Tsunashima, D. L. Long, H. N. Miras, D.

- Gabb, C. P. Pradeep, L. Cronin, *Angew. Chem.* **2010**, *122*, 117–120; *Angew. Chem. Int. Ed.* **2010**, *49*, 113–116.
- [7] a) J. Y. Niu, P. T. Ma, H. Y. Niu, J. Li, J. W. Zhao, Y. Song, J. P. Wang, *Chem. Eur. J.* **2007**, *13*, 8739–8748; b) J. P. Wang, H. Y. Niu, J. Y. Niu, *Inorg. Chem. Commun.* **2008**, *11*, 63–65.
- [8] Crystal data: for **1**, C₂₄H₆₈Cu₃K₃N₄Na₂Nb₁₁O₅₉, M_r = 2732.70, triclinic, P $\bar{1}$, *a* = 11.2911(18), *b* = 16.409(3), *c* = 22.773(4) Å, α = 90.088(2), β = 90.897(3), γ = 109.789(3)°, *V* = 3969.4(11) Å³, *Z* = 2, ρ_{calcd} = 2.283 g cm⁻³, μ = 2.583 mm⁻¹, *F*(000) = 2650, *GOF* = 1.035. A total of 20089 reflections were collected, 13762 of which were unique (*R*_{int} = 0.0312). *R*₁(*wR*₂) = 0.0706(0.1938) for 986 parameters and 13762 reflections [*I* > 2 σ (*I*)]. For **2**, C₂₀H₇₄Cu₃K₄N₄NaNb₁₁O₆₂, M_r = 2754.77, triclinic, P $\bar{1}$, *a* = 11.529(6), *b* = 16.053(8), *c* = 22.331(11) Å, α = 84.623(8), β = 83.139(9), γ = 70.677(8)°, *V* = 3866(3) Å³, *Z* = 2, ρ_{calcd} = 2.358 g cm⁻³, μ = 2.703 mm⁻¹, *F*(000) = 2666, *GOF* = 1.010. A total of 19784 reflections were collected, 13427 of which were unique (*R*_{int} = 0.0219). *R*₁(*wR*₂) = 0.0401(0.1191) for 967 parameters and 13427 reflections [*I* > 2 σ (*I*)]. Intensity data were collected at 296 K on a Bruker APEX-II CCD diffractometer for **1** and **2** using graphite-monochromated MoK α radiation (λ = 0.71073 Å). Routine Lorentz and polarization corrections were applied and an absorption correction was performed using the SADABS program. Direct methods were used to solve the structure and refined by full-matrix least-squares on *F*² using the SHELXTL-97 program package. All non-hydrogen atoms were refined anisotropically. CCDC-730010 (**1**) and 730011 (**2**) contain the supplementary crystallographic data for this paper. These data can be obtained free of charge from The Cambridge Crystallographic Data Centre via www.ccdc.cam.ac.uk/data_request/cif.
- [9] T. M. Che, V. W. Day, L. C. Francesconi, M. F. Fredrich, W. G. Klemperer, W. Shum, *Inorg. Chem.* **1985**, *24*, 4055–4062.
- [10] I. D. Brown, D. Altermatt, *Acta Crystallogr. Sect. B* **1985**, *41*, 244–247.
- [11] E. M. Villa, C. A. Ohlin, E. Balogh, T. M. Anderson, M. D. Nyman, W. H. Casey, *Angew. Chem.* **2008**, *120*, 4922–4924; *Angew. Chem. Int. Ed.* **2008**, *47*, 4844–4846.
- [12] a) D. L. Long, R. Tsunashima, L. Cronin, *Angew. Chem.* **2010**, *122*, 1780–1803; *Angew. Chem. Int. Ed.* **2010**, *49*, 1736–1758; b) Z. M. Zhang, Y. G. Li, S. Yao, E. B. Wang, Y. H. Wang, R. Clérac, *Angew. Chem.* **2009**, *121*, 1609–1612; *Angew. Chem. Int. Ed.* **2009**, *48*, 1581–1584; c) H. Q. Tan, Y. G. Li, W. L. Chen, D. Liu, Z. M. Su, Y. Lu, E. B. Wang, *Chem. Eur. J.* **2009**, *15*, 10940–10947; d) Y. Hou, X. K. Fang, C. L. Hill, *Chem. Eur. J.* **2007**, *13*, 9442–9447.
- [13] a) Y. H. Lin, D. J. Wang, Q. D. Zhao, M. Yang, Q. L. Zhang, *J. Phys. Chem. B* **2004**, *108*, 3202–3206; b) S. Z. Li, J. W. Zhao, P. T. Ma, J. Du, J. Y. Niu, J. P. Wang, *Inorg. Chem.* **2009**, *48*, 9819–9830.
- [14] K. Yu, Y. G. Li, B. B. Zhou, Z. H. Su, Z. F. Zhao, Y. N. Zhang, *Eur. J. Inorg. Chem.* **2007**, 5662–5669.
- [15] X. L. Wang, Y. F. Bi, B. K. Chen, H. Y. Lin, G. C. Liu, *Inorg. Chem.* **2008**, *47*, 2442–2448.
- [16] a) D. L. Long, E. Burkholder, L. Cronin, *Chem. Soc. Rev.* **2007**, *36*, 105–121; b) D. A. Judd, J. H. Nettles, N. Nevins, J. P. Snyder, D. C. Liotta, J. Tang, J. Ermolieff, R. F. Schinazi, C. L. Hill, *J. Am. Chem. Soc.* **2001**, *123*, 886–897; c) H. Thomadaki, A. Karaliota, C. Litos, A. Scorilas, *J. Med. Chem.* **2007**, *50*, 1316–1321; d) L. V. Lokeren, E. Cartuyvels, G. Absillis, R. Willem T. N. Parac-Vogt, *Chem. Commun.* **2008**, 2774–2776.
- [17] a) F. Tisato, C. Marzano, M. Porchia, M. Pellei, C. Santini, *Med. Res. Rev.* **2010**, *30*, 708–749; b) K. G. Daniel, P. Gupta, R. H. Harbach, W. C. Guida, Q. P. Dou, *Biochem. Pharmacol.* **2004**, *67*, 1139–1151.
- [18] M. Filowitz, R. K. C. Ho, W. G. Klemperer, W. Shum, *Inorg. Chem.* **1979**, *18*, 93–103.

Received: April 1, 2010
Published online: May 12, 2010